Temporal dynamics of tunneling: Hydrodynamic approach

G. Dekel and V. Fleurov*
Raymond and Beverly Sackler Faculty of Exact Sciences, School of Physics and Astronomy, Tel-Aviv University, Tel-Aviv 69978, Israel

A. Soffer and C. Stucchio
Department of Mathematics, Rutgers University, New Brunswick, New Jersey 08903, USA
(Received 21 December 2006; published 19 April 2007)

We use the hydrodynamic representation of the Gross-Pitaevskii and nonlinear Schrödinger equations in order to analyze the dynamics of macroscopic tunneling processes. We observe a tendency to wave breaking and shock formation during the early stages of the tunneling process. A blip in the density distribution appears on the outskirts of the barrier and under proper conditions it may transform into a bright soliton. Our approach, based on the theory of shock formation in solutions of the Burgers equation, allows us to find the parameters of the ejected blip (or soliton if formed), including the velocity of its propagation. The blip in the density is formed regardless of the value and sign of the nonlinearity parameter. However, a soliton may be formed only if this parameter is negative (attraction) and large enough. A criterion is proposed. An ejection of a soliton is also observed numerically. We demonstrate, theoretically and numerically, controlled formation of a soliton through tunneling. The mass of the ejected soliton is controlled by the initial state.

DOI: 10.1103/PhysRevA.75.043617 PACS number(s): 03.75.Kk, 82.20.Xr, 05.90.+m

I. INTRODUCTION

The recent advances in experiments on real Bose-Einstein condensates (BECs) [1–3] and nonlinear optical waves [4,5] have generated a huge body of works on the theoretical side based on the Gross-Pitaevskii (GP) [6,7] (see also Refs. [8–10]) or nonlinear Schrödinger (NLS) equation [9,11]

$$i\hbar\frac{\partial}{\partial t}\Psi(\mathbf{r},t)=\left[-\frac{\hbar^2}{2m}\nabla^2+U(\mathbf{r})+\lambda|\Psi(\mathbf{r},t)|^2\right]\Psi(\mathbf{r},t). \quad (1)$$

The dynamics of solutions of this equation is very complex and rich. The phenomena of coherence [12], macroscopic tunneling [14,15], vortex formation [16–21], instabilities, focusing, and blowup are all concepts related to the *nonlinear* nature of the systems. Dark solitons, or kinkwise states—i.e., states with dynamically stable propagating density minima—are expected in condensates with repulsive interactions. They have been predicted for one-dimensional BECs [22–25] and may occur in higher dimensions as well. There have been several suggestions for techniques to engineer dark solitons in BECs [26], and these were indeed successfully created and observed [27,28]. The two groups used far-off-resonance laser beam pulses to shift the matter wave phase, thus creating density minima.

As for bright solitons, the situation is more subtle, since in such systems instability of the gas is unavoidable above a critical particle number where the zero-point kinetic energy does not suffice to balance the collapse mechanism. The latter renders the system to behaviors which deviate significantly from the mean-field validity range. The critical number has been calculated theoretically for ^{7}Li to be $N_{cr}=1400$ [29,30], which is consistent with the experimental measurements. A condensate with a limited number of atoms, however, can be stabilized by confinement in a trap. In 1995, the first evidence for a BEC in ^{7}Li atomic gas with attractive interactions was reported [3]. Later that year, the stability of solitons created in condensates in a small harmonic trap, constrained to one-dimensional (1D) motion, was predicted from numerical calculations [31]. For the 3D case, however, the solitons were predicted to be stable for modest ranges of nonlinearities. In 1998 an analytic solution was obtained for BEC bright soliton creation in an asymmetric, cigar-shaped trap. It was then shown that the solitons do not expand when confinement in one direction is lifted [32]. A major stepping stone was undoubtedly the production and observation by two experimental groups [33,34] of bright solitons in ultracold ^{7}Li gas, released from a one-dimensional trap. Both groups reported propagation without dispersion over macroscopic distances. The latter group also observed propagation of a soliton train.

The question of BEC bright soliton formation, stability, and dynamics is far from being solved and the ongoing research is very active. Ways to stabilize two-dimensional BEC solitons by using spatial modulation of the interaction strength [35] and by using rapid oscillations between repulsive and attractive interactions [36] were suggested. The existence of vortex solitons in periodic potentials (optical lattices) was revealed in Refs. [37–39]. Exact solutions for the dynamics of 1D trapped BEC bright solitons with a time-dependent interaction strength were found in Ref. [40]. Interference of tunneling BEC matter waves in an optical array was observed [41] and the existence of bounce solutions in macroscopic tunneling was investigated in Ref. [42]. The dynamics of an initially nonuniform bright soliton was studied in [43] as was friction and diffusion of bright solitons by the thermal cloud [44]. The dynamics of a bright BEC soliton in an expulsive potential was investigated in [45]. Finally, pulsed macroscopic quantum tunneling of BECs is expected, which is induced by the scattering of solitons on the Gaussian potential barrier [13].

Remarkably, many similar phenomena are observed in light propagation, when we have to turn to electromagnetic

*Electronic address: fleurov@post.tau.ac.il

wave propagation and penetration into media with different refraction indices instead of matter wave dynamics. Atomic correlations now correspond to the coherence of laser light, while many-body (mean-field) interactions correspond to Kerr nonlinearity. Examples of parallel dynamics include soliton formation and modulation instability [34] in the focusing (attractive) case and dark solitons [46] and dispersive shock waves in the defocusing (repulsive) case [47,48]. Multispecies condensates relate to multicomponent, or vector, beams of light, while periodic potentials for both the atomic and photonic systems have been demonstrated using standing light waves [4,49]. Of course, there are also significant differences between the two systems, particularly when atomic excitations and quantum (versus classical) statistics are involved. In these cases, too, it is useful to contrast optics with BECs in order to better understand the underlying dynamics of both.

Most of the theoretical analysis of the works mentioned above have so far been dealt with by a combination of numerical schemes (e.g., Ref. [13,14]) and finite-dimensional phenomenological models. Furthermore, all assume long-time existence of the solitons in the gas. None has considered the problem of tracing the mechanisms responsible for the actual formation of the soliton in the course of tunneling. In other words, the problem of the short-time dynamics of tunneling has so far not been addressed. The tendency to shock formation and creation of solitons at the early stages of the tunneling process is another aspect of the theory presented in this paper. As we shall see below an interesting aspect of this process is the possibility to control such soliton parameters as mass, geometrical factors, and velocity.

The hydrodynamic formulation for the Schrödinger equation was originally proposed in Ref. [50]. A similar approach is also well known in linear and nonlinear optics (see, e.g., [51,52]). Recently a hydrodynamic formalism received much attention [53–57] as a useful tool for analyzing the GP-NLS equation as well as other systems like the fractional quantum Hall effect [58]. The time-independent problem has been studied as far back as the early 1950s [59]. We apply this approach to one-dimensional systems. Its generalization to higher dimensions is straightforward, although it may require special consideration of vortices.

We study nonlinear phenomena in the macroscopic tunneling of a BEC gas or optical systems. Employing the hydrodynamic representation we analyze the time-dependent GP-NLS equation (1) and obtain the dynamics of a trapped droplet tunneling through a barrier both on the short and long time scales. We predict a splitting process, in which a blip in the density distribution is formed at short times outside the confining potential. We find the conditions under which it may evolve into an outgoing bright soliton. Our approach allows for an analytical calculation of its parameters, including the velocity and energy. We also show numerical evidence for the blip and soliton formation. This theory allows one to design a structure in which we can fully control the parameters of the ejected soliton, including its velocity and mass fraction split off of the initially trapped BEC. The latter observation also indicates a way to extract a stable BEC soliton out of a less stable one. These are feasible processes. Their experimental implementation may be carried out, e.g., by measuring light propagation in samples with spatially modulated refraction index [60,61].

II. GENERAL APPROACH

We consider here the 1D dynamics of BEC in an external potential $V_{ext}(x)$. Equation (1) for a complex wave function $\Psi(x,t)$ describing the system may be equivalently written as two equations for two real functions: the continuity equation

$$\frac{\partial}{\partial t}\rho(x,t) + \frac{\partial}{\partial x}[\rho(x,t)v(x,t)] = 0 \tag{2}$$

for the particle density distribution $\rho(x,t)=|\Psi(x,t)|^2$ and the Euler-type equation

$$\frac{\partial}{\partial t}v(x,t) + v(x,t)\frac{\partial}{\partial x}v(x,t) = -\frac{1}{m}\frac{\partial}{\partial x}V_{eff}(x,t) \tag{3}$$

for the velocity field $v(x,t)=\frac{\partial}{\partial x}\phi$, where ϕ is the phase of wave function and the effective potential

$$V_{eff}(x,t) = V_{ext}(x) + V_{qu}(\{\rho(x,t)\}) + \lambda\rho(x,t) \tag{4}$$

includes the quantum potential

$$V_{qu}(\{\rho(x,t)\}) = -\frac{\hbar^2}{2m}\frac{1}{\sqrt{\rho(x,t)}}\frac{\partial^2}{\partial x^2}\sqrt{\rho(x,t)}. \tag{5}$$

The latter is often also called quantum pressure (QP). The effective potential (4) is a functional of the density distribution $\rho(x,t)$ and may vary in time so that generally the two equations should be analyzed together.

Sometimes we have information about the density distribution and may solve Eq. (3) separately. The diffusion term

$$\frac{\zeta}{2m}\frac{\partial^2}{\partial x^2}v(x,t)$$

on the right-hand side of Eq. (3) is introduced as a singular perturbation [62] which ensures its dissipative regularization,

$$\frac{\partial}{\partial t}v(x,t) + v(x,t)\frac{\partial}{\partial x}v(x,t) = \frac{\zeta}{2m}\frac{\partial^2}{\partial x^2}v(x,t) - \frac{1}{m}\frac{\partial}{\partial x}V_{eff}(x,t). \tag{6}$$

We expect a tendency to formation of a shock wave in the velocity and density distributions. It is well known that the Burgers equation with the diffusion term has steplike solutions, which survive even if the "diffusion" coefficient ζ tends to zero. However, this type of solution does not appear if $\zeta=0$ from the very beginning [see, e.g., Eqs. (4.1) and (4.2) in Ref. [57]]. Therefore we first analyze Eq. (6) for finite values of the coefficient ζ and then take the limit $\zeta \to 0$ in the final results.

We may now apply the Cole-Hopf transformation

$$v(x,t) = -\frac{\zeta}{m}\frac{\varphi_x(x,t)}{\varphi(x,t)}, \tag{7}$$

so that the new function $\varphi(x,t)$ satisfies the linear diffusion equation with a source:

$$\varphi_t(x,t) = \frac{\zeta}{2m}\varphi_{xx}(x,t) + \frac{1}{\zeta}V_{eff}(x,t)\varphi(x,t). \tag{8}$$

The Green function of Eq. (8) can be represented by the Wiener path integral

$$G(x,x_0,t,0) = \int_{x_0,0}^{x,t} D[x(\tau)]e^{-(1/\zeta)S([x(\tau)];t,0)}, \tag{9}$$

where

$$S([x(\tau)];t,0) = \int_{t_0}^{t}\left[\frac{m}{2\zeta}\left(\frac{dx(\tau)}{d\tau}\right)^2 d\tau - V_{eff}(x(\tau),\tau)\right]d\tau$$

has the form of an action for a particle with the mass m moving along a path in the potential V_{eff}. Distinguishing as usual the contribution of the classical path $x_c(\tau)$ we get the saddle point approximation for the Green function,

$$G(x,x_0;t,0) = F(t)e^{-(1/\zeta)S([x_c(\tau)];t,0)}. \tag{10}$$

This approximation leads in fact to exact results in the limit $\zeta \to 0$. In particular the preexponential factor $F(t)$ plays no role in this limit. We look for the solution $\varphi(x,t)$ of Eq. (8), which at $t=0$ has the form

$$\varphi_0(x) = e^{-(1/\zeta)S_0(x)}.$$

Returning to the Cole-Hopf transformation (7) we understand that the function $S_0(x)$ must be chosen to satisfy the condition

$$v_0(x) = \frac{1}{m}\frac{dS_0(x)}{dx},$$

where $v_0(x)$ is the initial velocity field at $t=0$ of the original physical problem.

The solution of Eq. (8) with this initial condition then reads

$$\varphi(x,t) = \int_{-\infty}^{\infty} dx' G(x,x',t)\varphi_0(x')$$

$$= F(t)\int_{-\infty}^{\infty} dx' e^{-(1/\zeta)[S_0(x')+S(x,x',t)]}. \tag{11}$$

The integration in Eq. (11) is carried out around the saddle point defined by

$$\frac{\partial S(x,x',t)}{\partial x'} = -mv_0(x'), \tag{12}$$

so that

$$\varphi(x,t) \propto e^{-(1/\zeta)[S_0(\bar{x}(x,t))+S(x,\bar{x}(x,t),t)]}, \tag{13}$$

where $\bar{x}(x,t)$ is obtained by solving Eq. (12) with respect to x' for a given x and t. Substituting solution (13) into Eq. (7), using the initial condition (12), and taking the limit $\zeta \to 0$ one gets the velocity field in the form

$$v(x,t) = \frac{\partial S(x,\bar{x}(x,t),t)}{\partial x}.$$

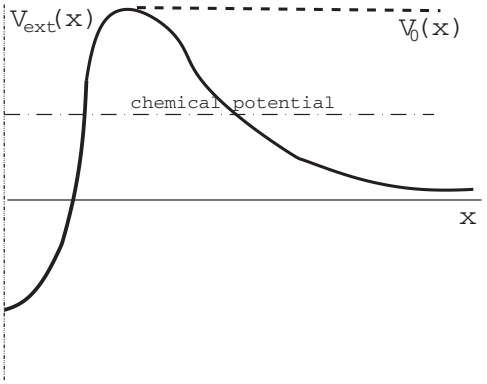

FIG. 1. The right half view of the trap potential $V_{ext}(x)$ keeping the droplet. The dashed line shows the auxiliary potential $V_0(x)$ which differs from $V_{ext}(x)$ only to the right from the top of the potential barrier. The dash-dotted line corresponds to the chemical potential μ for a given number N of particles.

This result has a simple interpretation. As mentioned above the function $S(x,\bar{x},t)$ is the mechanical action of a particle (to be called "tracer" below) with the mass m moving from point $\bar{x}$ to x during time t in the potential V_{eff}. $v_0(\bar{x})$ is its initial velocity. In other words, we have to solve the following equivalent problem. At a time t an observer measures the velocity field in an "effective fluid" flowing in the external potential $V_{eff}(x,t)$ under the condition that the initial velocity field be $v_0(x)$. The possible compressibility of the fluid is accounted for by the dependence of the quantum pressure and, hence, $V_{eff}(x)$ on the density distribution. If the measurement is carried out in the point x, the observer sees the tracer, which has started at time 0 from point $\bar{x}$ with velocity $v_0(\bar{x})$. The question is what the tracer's velocity measured by the observer is. Solving this problem we obtain the velocity distribution of the fluid flowing in the effective potential (16), which according to the above procedure coincides with the velocity field of the actual quantum fluid. Below we analyze this problem for a model choice of the effective potential V_{eff} and obtain the velocity field as a function of time t.

III. MODEL

A. Adiabatic approximation

We consider here tunneling escape from the one-dimensional potential trap, Fig. 1.

Tunneling of a particle with energy μ from the trap is characterized by the time of tunneling escape:

$$\tau_{tun} \sim \nu^{-1}e^{\lambda_{tun}},$$

where ν is the frequency of oscillations within the trap and

$$\lambda_{tun} = \frac{1}{\hbar}\int_a^b dx\sqrt{2m[V_{ext}(x)-\mu]}$$

is the tunneling integral of the classically forbidden under-barrier region (a,b). There is also another important characteristic of tunneling which is the time τ_{tr} needed to traverse

the underbarrier region [63]. This duality in tunneling characterization was first introduced in Ref. [64] and has been dealt with in many works since [63,65–67]. The traversal time is a matter of intensive research and has attracted attention for both fundamental and technological reasons. Among many possible definitions of the traversal time the "semiclassical" traversal time

$$\tau_{tr} = \sqrt{\frac{m}{2}} \int_a^b dx \frac{1}{\sqrt{V_{ext}(x) - E}} \tag{14}$$

proposed in Ref. [67] is most popular and will be used below. It is obtained by modulating the potential barrier with a small cosine perturbation and finding the traversal time as the crossover between high- and low-frequency behaviors.

In what follows we embrace the definition (14) for the traversal time and rely on the additional important observation that the density field varies on the time scale τ_{tun}, whereas the velocity field varies on the time scale τ_{tr} [56]. The inequality $\tau_{tr} \ll \tau_{tun}$, valid for typical barriers, assumes the dynamics of the velocity field at virtually constant density. We may therefore use this assumption in order to apply the adiabatic approximation in the first iteration. The second step will be to calculate the time dependence of the density, $\rho(x,t)$, for the time-dependent velocity field found in the first iteration. The former will end, by definition, when changes in the density field become significant.

We consider now a droplet trapped in the potential $V_{ext}(x)$ from which it escapes due to tunneling through the potential barrier. In order to define the initial density distribution $\rho_0(x)$ we introduce an auxiliary confining potential $V_0(x)$ from which tunneling is impossible and a stationary state is formed. This potential coincides with $V_{ext}(x)$ for small x up to the top of the potential barrier but differs for larger x (dashed line in Fig. 1). The density distribution $\rho_0(x;N)$ of the stationary state in the auxiliary potential $V_0(x)$ is obtained from Eq. (3) at $v(x,t)=0$, which becomes

$$\left[V_0(x) - \frac{\hbar^2}{2m} \frac{\partial^2}{\partial x^2} + \lambda \rho_0(x;N) \right] \sqrt{\rho_0(x;N)} = \mu(N) \sqrt{\rho_0(x;N)}. \tag{15}$$

Equation (15) is in fact the stationary GP-NLS equation with the potential $V_0(x)$ and determines therefore the initial density distribution $\rho_0(x;N)$. Here $\mu(N)$ is the chemical potential. The calculations are carried out for a given total number N of particles in the trap.

Using Eq. (15) for $\rho_0(x;N)$ we get that the effective potential in Eq. (6) for a given number $N(t)$ of particles becomes

$$V_{eff}(x) = V_{ext}(x) - V_0(x) + \mu + V_{qu}(\{\rho(x,t)\}) - V_{qu}(\{\rho_0(x;N(t))\}) + \lambda[\rho(x,t) - \rho_0(x;N(t))]. \tag{16}$$

The number of particles, $N(t)$, in the trap may vary slowly with time. Generally the effective potential follows the variation of the density distribution. However, the adiabatic approximation implies that the density field varies much slower than the velocity field. It ensures also that the QP follows also the change of the total number of particles in the trap in the course of time, which is reflected by a slow variation of the chemical potential μ with slowly changing number of particles, $N(t)$ [56]. Hence we may, to within a good precision, assume that $\rho(x,t)=\rho_0(x;N(t))$ in Eq. (16), meaning that

$$V_{eff}(x) = V_{ext}(x) - V_0(x) - U_0, \tag{17}$$

where U_0 is the asymptotic value of the difference $V_{ext}(x) - V_0(x)$ at large x. Hence this parameter is just the height of the barrier. The chemical potential is dropped under the derivative over the coordinate x in Eq. (6), and the constant $-U_0$ is introduced for the sake of convenience so that $V_{eff}(x) \to 0$ at $x \to \infty$. Therefore the effective potential is shifted by the time-independent difference U_0 of the actual potential forming the trap and the auxiliary potential used to form the initial density distribution (at large $|x|$).

The effective potential (17) has a bell-like shape, being zero at $x \to \pm\infty$ and reaching its maximum value of about U_0 at $x=0$. Its width is related to the barrier width. We plan at this stage to follow an analytical approach to the problem. For this sake it is worthwhile to choose a model shape, which will properly reflect the above-mentioned properties of the effective potential and will be simple enough to carry out the calculations. At a later stage we will carry out straightforward numerical calculations and compare the results. This aim can be achieved by choosing the effective potential (17) in the form

$$V_{eff}(x) = \frac{U_0}{\cosh^2 \alpha x}, \tag{18}$$

which includes the height U_0 of the barrier and another parameter α which characterizes the inverse width of the barrier. Since we start from the stationary state $\rho_0(x;N)$ as the initial density distribution, we also assume the zero initial velocity field $v_0(x)=0$. The effective potential (18) is time independent so that we deal with an "adiabatically" incompressible flow. The compressibility—i.e., variations of $\rho(x,t)$ and, hence, V_{eff} with time—can be accounted for in higher iterations.

According to the analysis in Sec. II we have to calculate the velocity field $v(x,t)$ of the equivalent fluid at a given point x and time t with the initial conditions described above. For this sake we consider a fluid tracer which starts moving at a point $\bar{x}$ at initial time $t=0$ with initial velocity $v(x,0)=0$. The initial energy of the tracer,

$$\bar{\varepsilon} = \frac{U_0}{\cosh^2 \alpha \bar{x}}, \tag{19}$$

is conserved in the Lagrange coordinates when we follow the tracer along the path of its motion. Hence at the point of observation x (which is a static Euler coordinate) and at the time of observation t it becomes

$$\bar{\varepsilon} = \varepsilon(x,t) \equiv \frac{U_0}{\cosh^2 \alpha x} + \frac{m v^2(x,t)}{2}. \tag{20}$$

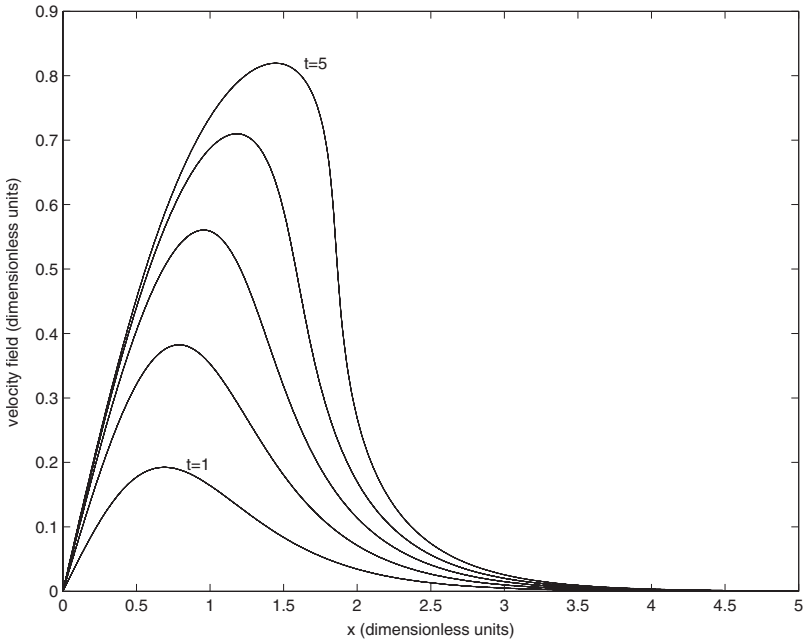

FIG. 2. Velocity profiles (in the $\sqrt{2U_0/m}$ units) $\tilde{v}(\xi)$ for increasing times $\tau=1,2,3,4,5$.

Equations (19) and (20) allow us to connect the starting point $\bar{x}$ of the tracer motion with the velocity field measured at time t at point x.

The tracer, which has started from point $\bar{x}$ with energy ε, reaches the point of observation, x, after time

$$t = \int_{\bar{x}}^{x} \frac{1}{\sqrt{\frac{2}{m}\left(\varepsilon - \frac{U_0}{\cosh^2 \alpha x}\right)}} dx. \tag{21}$$

This integral together with the initial condition (19) implicitly defines the energy $\varepsilon(x,t)$ of the tracer observed at point x at time t. Calculating the integral in Eq. (21) we arrive at the equation

$$F(w;\xi,\tau) \equiv 2 - w + 2\sqrt{1-w} - w \exp\left\{\frac{\tau}{\sqrt{w \sinh^2 \xi + 1}}\right\} = 0, \tag{22}$$

where

$$w = \frac{U_0 - \varepsilon}{\varepsilon \sinh^2 \xi},$$

with $0 \leqslant w \leqslant 1$. Here we use dimensionless time, $\tau = 2t\sqrt{2U_0\alpha^2/m}$, and space, $\xi = \alpha x$, coordinates. It is worth noting that the time scale $\sqrt{m/2U_0\alpha^2}$ is of the order of the traversal tunneling time (14) and appears as a natural scale for the time variation of the velocity field in the course of tunneling.

B. Velocity field

Equation (22) is solved with respect to w, so that we get the quantity $\varepsilon(\xi,\tau)$ at a given ξ and τ. Then we obtain the velocity field

$$v(\xi,\tau) = \sqrt{\frac{2}{m}\left[\varepsilon(\xi,\tau) - \frac{U_0}{\cosh^2 \xi}\right]}.$$

Equation (22) is nonlinear and may have more than one solution. One can find the critical time $\tau_c = 5.55$ and position $\xi_c = 2.005$ from the condition that the function $F(w;\xi,\tau)$ in Eq. (22) become zero simultaneously with its first and second derivatives. Then, for $\tau < \tau_c$, Eq. (22) has only one solution at each value of the coordinate ξ. At longer times $\tau > \tau_c$, there is a finite range of ξ values at $\xi > \xi_c$, where Eq. (22) has three solutions.

The appearance of three solutions corresponds to a breakdown of the wave (see, e.g., discussion in Ref. [68]) and to formation of a shock wave. In the critical region the procedure as outlined in Sec. II should be amended. It means in fact that Eq. (12) has several solutions and, hence, the integrand in Eq. (11) has several saddle points. The saddle point, at which the action $S(x,x',t)$ is the smallest will determine the actual velocity field in the limit $\zeta \to 0$.

The velocity field at $\tau \leqslant \tau_c$ is shown in Fig. 2. A blip is formed on the outskirts of the barrier, which then approaches the wave breakdown at $\tau = \tau_c$, Fig. 3. This type of behavior is characteristic of shock wave formation. We do not follow the further evolution of the velocity field since we have stretched the adiabatic approximation to its limit. In fact, we should consider this result as the first iteration and calculate the evolution of the density field by means of the continuity equation (2), which may introduce corrections to the effective potential (18) in the region where the shock wave is going to be formed.

Although the fully developed shock with a sharp step in the density distribution would be an artifact of the approximation of incompressible flow used to calculate the velocity field, its analysis allows for an estimate of the speed of blip propagation. Solving simultaneously the equations

$$F(w;\xi,\tau) = 0, \quad \frac{\partial F(w;\xi,\tau)}{\partial \xi} = 0,$$

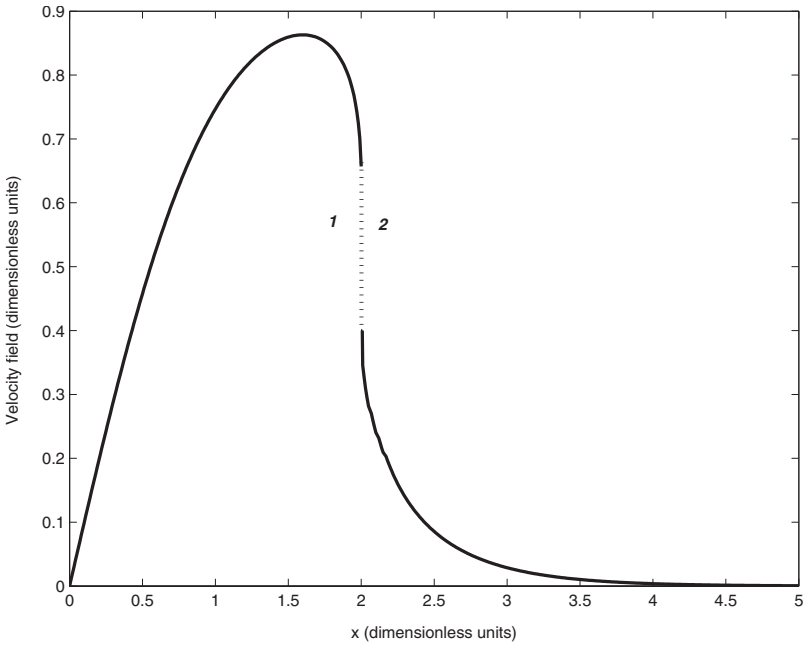

FIG. 3. Velocity profile (in the $\sqrt{2U_0/m}$ units) at $\tau=\tau_c$ where breakdown of the wave occurs.

at a given time $\tau > \tau_c$, we find two values of the coordinate ξ between which the shock occurs. Using the fact that w is small in this region, we obtain the upper limit of the blip velocity:

$$v_b = \sqrt{\frac{2U_0}{m}}.$$

It is worth emphasizing that v_b is of the order of the velocity with which the tunneling particles traverse the classically forbidden barrier region.

C. Density field

The development of a blip in the velocity field results in a local increase of the density at $\tau < \tau_c$ (see Fig. 4). The variation of $\rho(x,t)$ near the blip is found from the continuity equation (2) assuming similarly to Ref. [56] that in the region where the blip is formed (i.e., outside the trap) the initial density distribution is

$$\rho_0(x) = \tilde{\rho} e^{-\beta x},$$

where $\beta = 2\sqrt{2m(U_0-\mu)}/\hbar$ and $\tilde{\rho}$ is a constant. We solve the equation

$$\frac{\partial \rho(x,t)}{\partial t} = -\frac{\partial}{\partial x}[\rho_0(x,t)v(x,t)], \tag{23}$$

where $v(x,t)$ is the time-dependent velocity field calculated in Sec. III B. The relative variation of the density,

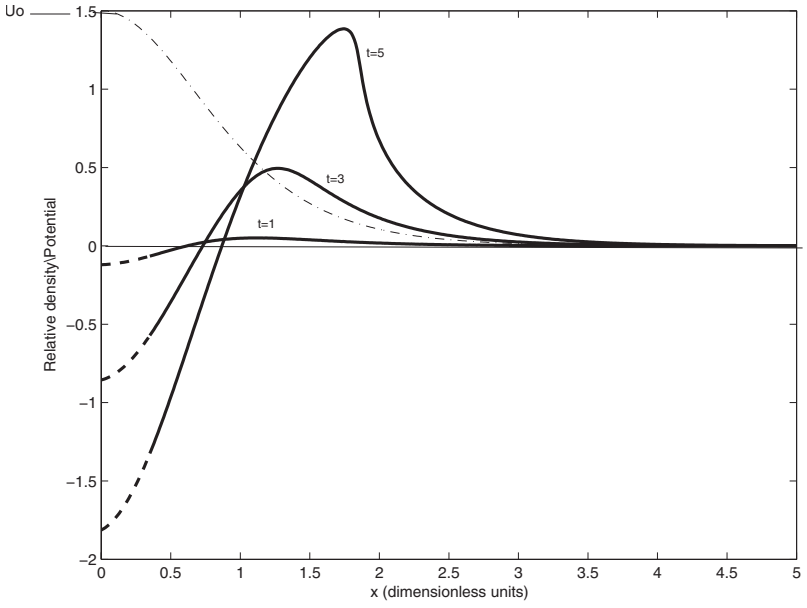

FIG. 4. The blip in the density distribution at $\tau=1,3,5$ for $\beta=0.25\alpha$. The lines become dashed inside the trap where the calculation errors may be large. The shape of the effective potential (out of scale) is shown by the dash-dotted line.

$$\rho_{rel}(\xi,\tau) \equiv \frac{\rho(\xi,\tau)-\rho_0(\xi)}{\rho_0(\xi)} = \int_0^\tau d\tau' \frac{1}{2}\left[\frac{\beta}{\alpha}v(\xi,\tau') - \frac{\partial v(\xi,\tau')}{\partial \xi}\right], \tag{24}$$

is obtained by integrating Eq. (23) over time.

The calculated distribution $\rho_{rel}(\xi,\tau)$ of the relative density variation is shown in Fig. 4 at several times $\tau < \tau_c$. The blip in the density propagates with the velocity v_b, leaving a depleted region behind. Although the depletion is a real effect, the approximate procedure leads to a too strong depletion inside the trap as shown by the dashed lines, meaning that we cross the applicability limits of the procedure.

We clearly see a tendency to wave breakdown and formation of a shock at times approaching the critical time τ_c. This, however, does not happen, and the wave does not break down and form a shock in the density field $\rho(x)$, since such a development is inhibited by the quantum potential (5). The latter contains the second derivative of the density which may become large in the area of the blip formation even though the absolute value of $\rho_{rel}(\xi,\tau)$ may be still small. The corresponding correction to the effective potential (16) prevents the sharp shock formation.

Formation of a soliton

At $\tau=3$ the blip moves in a weak potential in the outskirts of the trap and we deal with a new problem of a packet propagating with a the velocity $\sim v_b$, which may or may not transform into a soliton. A direct comparison shows that the shape of the blip is close to that of the soliton. The latter is formed if the blip energy E_{blip} in its center-of-mass coordinate system is negative (e.g., Ref. [69] and references therein). This condition may be fulfilled only if the interaction parameter $\tilde{\lambda}=2m\lambda/\hbar^2$ is negative (attractive interaction). Calculating E_{blip} by means of the Gross-Pitaevskii surface energy functional we get the inequality

$$|\tilde{\lambda}|\tilde{\rho} > \left(12.95\alpha^2 + 0.123\frac{mU_0}{2\hbar^2}\right); \tag{25}$$

i.e., for each value of U_0 and α there is a lower limit for the interaction strength above which a soliton may be formed. Its width is about twice the width of the trap, and it contains about 10% of the initial packet. For the typical parameters of the currently available systems, $m=7$ amu$=11.69\times10^{-27}$ kg (for Li atoms), $U_0=10^{-33}$ J, $\alpha=10^4$ m^{-1}, and $\tilde{\rho}=10^{16}$ m^{-3}, we get $|\tilde{\lambda}|>2.38\times10^{-7}$ m. Finally, a soliton is formed if the interaction coefficient satisfies the condition $|\lambda|>0.73\times10^{-49}$ J m^3, which is typically fulfilled and has been measured experimentally (see, e.g., [33]).

The condition (25) is necessary for the soliton formation. In the one-dimensional case the soliton, if formed, remains stable. In the two- and three-dimensional cases the condition (25) by itself does not guarantee the survival of such a soliton, which may be unstable with respect to the collapse at $\lambda<0$. For $\lambda\geq0$ the soliton cannot exist and the blip disperses. However, it is important to emphasize that we consider here very-short-time processes so that the blip formation can be observed before the possible instabilities become fully developed. The blip formation at short times takes place for any sign of the interaction term or even in the case of a more complicated functional dependence. For example, a self-saturating nonlinearity is considered in nonlinear optics (see, e.g., [46]) so that the collapse problem loses its acuteness. Another possibility is to use a positive higher-power term with a small coefficient [9] which also removes the blowup.

It is also emphasized that in the case of a weaker than in Eq. (25) negative (attractive), zero, or even positive (repulsive) interaction parameter λ the soliton is not formed; however, the solitonlike blip in the density will be always formed and propagate far away from the trap (many hundreds of barrier widths) before being dispersed.

D. Numerical solution

We may observe as soliton is formed and ejected in the course of tunneling also in the direct numerical solution of the GP-NLS equation (1) carried out using the program KITTY [70]. Varying the trap potential in a wide range of its parameters we were always able to observe the formation of the blip. Here we present an example of the computation carried out for the GP-NLS Hamiltonian

$$H = -\frac{1}{2}\nabla^2 + V(x) - \frac{1}{2}|\Psi(x,t)|^2,$$

where

$$V(x) = \frac{9}{8}\left(1+\frac{x^4}{25}\right)\exp\left(-\frac{x^4}{35}\right),$$

with the initial wave function

$$\Psi(x,0) = \frac{3\sqrt{2}}{4}\frac{1}{\cosh(3x/4)}.$$

We may construct the effective potential (4) for this model and roughly fit it to the model choice (18) with $\alpha=0.5$ and $U_0=1.2$. Then we get $1/\sqrt{8U_0\alpha^2/m}=0.65$ as the time unit in our above analysis in Sec. III. It means that the reduced units used in this numerical calculation differ not essentially from those applied above.

Formation of a blip with a negative energy outside the potential barrier at short times is shown in Fig. 5, whereas Fig. 6 shows its propagation at longer times. One can clearly see two parallel lines showing the core of the blip, which slowly oscillates approaching the soliton shape. It is worth emphasizing that the characteristics of the soliton, obtained numerically, are quite close to those obtained in our above analysis, including the time ($\simeq6$) and location of the blip formation ($\simeq6$) and the velocity of its propagation $\simeq0.8$. These numbers are recalculated with the units compatible with the analysis in the main body of the paper. We see that the numbers obtained in the numerical procedure are only a

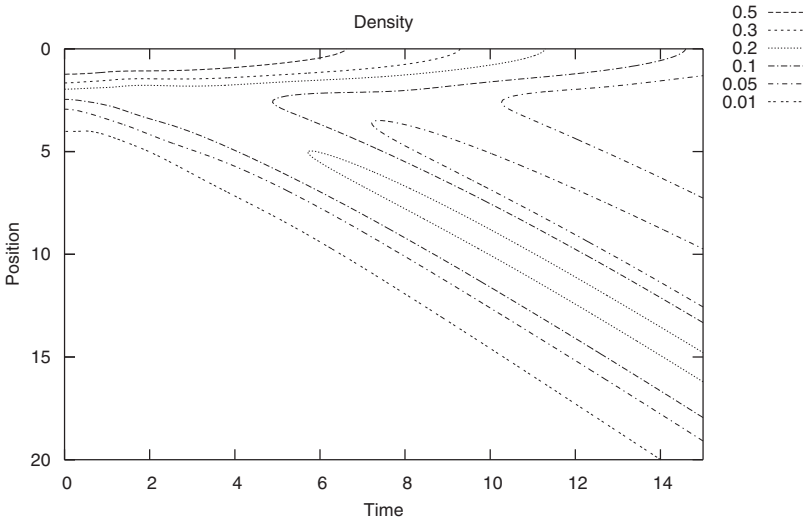

FIG. 5. Contour plot of the density distribution evolving with time. The figure shows the formation of a blip outside the barrier at short times.

little bit larger (smaller for the velocity) than those obtained in the analytical procedure. Keeping in mind a rather rough approximation made by choosing the shape (18), this quantitative agreement is quite impressive.

IV. CONCLUSIONS

Using the fluid dynamics paradigm, we have analyzed the GP-NLS equation and demonstrated the phenomenon of shock formation in the course of tunneling short-time dynamics. It results in the formation and ejection of a blip in the density field of the outgoing mass. It is emphasized that the process takes place at early stages of tunneling and is not dependent on the particular shape of the nonlinear term in the GP-NLS equation. When the suitable conditions are fulfilled the blip may later on transform into a bright soliton. We propose a technique which allows for analysis of the short-time dynamics of tunneling processes and provides us with a insight to the fundamental problem of macroscopic tunneling.

We believe that the conclusion of this paper can be straightforwardly verified experimentally both in BEC tunneling or in nonlinear optics measurements. By engineering a trap with the proper parameters we control the tunneling process and formation of bright solitons. The blip splits from a larger and narrower and thus less stable trapped packet; therefore, a general approach of ensuring stability by the BEC tunneling is presented.

Although the model considered here assumes that a BEC droplet is bound within a trap, the blip formation in the course of tunneling is the property of the barrier and is observed for other initial states as well; e.g., numerics show a similar effect in 2D systems.

The model we analyzed can be implemented experimentally both for BEC and optical soliton devices. The latter requires a quite simple setup of an optical fiber, with a spatially modulated refraction index, constituting the trap and its outings. As the light propagates, a blip should be detected near the trap outings, which escapes towards the sides of the fiber and develops into a soliton. By controlling the initial state—i.e., the initial mass of the BEC droplet or light intensity—we may obtain a "soliton gun" for the prescribed mass and velocity of the ejected solitons. Our approach applies to other nonlinear soliton dynamical effects—e.g.,

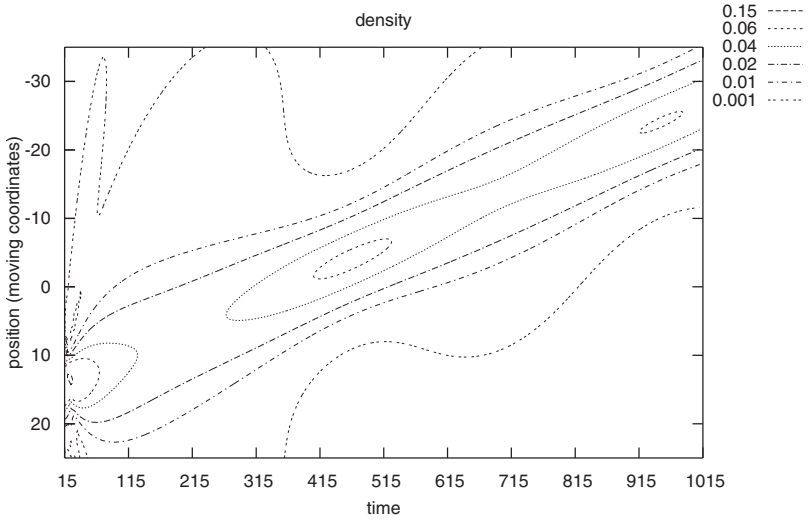

FIG. 6. Contour plot of the density distribution evolving with time. The figure shows propagation of the blip and its gradual conversion into a soliton at long times. The lower graph uses the frame, which moves with the velocity $v=1.047$ and follows the blip.

soliton slicing [71] (by a potential bump) and generally solitons interacting with a potential. Another important example may be the dynamics of nonlinear models of fission (see, e.g., [72]).

Note added in proof. Recently, our attention was drawn to the work of L. D. Carr and Y. Castin [73] that studies dynamics and stability of a bright BEC soliton in an expulsive potential.

ACKNOWLEDGMENTS

The authors are indebted to S. Flach, S. Bar-Ad, J. Brand, and J. Fleischer for useful comments. A.S. and G.D. are partially supported by the NSF. V.F. and G.D. are supported by Israeli Science Foundation, Grant No. 0900017. V.F. was partially supported by NSF Grant No. DMR-0442066 during his stay at Rutgers.

[1] M. H. J. Anderson, J. R. Ensher, M. R. Matthews, and C. E. Wieman, Science **269**, 198 (1995).
[2] K. B. Davis, M.-O. Mewes, M. R. Andrews, N. J. van Druten, D. S. Durfee, D. M. Kurn, and W. Ketterle, Phys. Rev. Lett. **75**, 3969 (1995).
[3] C. C. Bradley, C. A. Sackett, J. J. Tollett, and R. G. Hulet, Phys. Rev. Lett. **75**, 1687 (1995).
[4] J. W. Fleischer, M. Segev, N. Efremidis, and D. B. Christodoulides, Nature (London) **422**, 6928 (2003).
[5] G. P. Agrawal, *Nonlinear Fiber Optics*, 2nd ed. (Academic Press, San Diego, 1995).
[6] L. P. Pitaevskii, Sov. Phys. JETP **13**, 451 (1961).
[7] E. P. Gross, J. Math. Phys. **4**, 195 (1963).
[8] S. Inouye, M. R. Andrews, J. Stenger, H. J. Miesner, D. M. Stamper-Kurn, and W. Ketterle, Nature (London) **392**, 151 (1998).
[9] C. Sulem and P. L. Sulem, *The Nonlinear Schrödinger Equation* (Springer-Verlag, New York, 1999).
[10] E. H. Lieb and J. Yngvason, Phys. Rev. Lett. **80**, 2504 (1998); E. H. Lieb, R. Seiringer, and J. Yngvason, Phys. Rev. A **61**, 043602 (2000).
[11] Equation (1) is written as an equation for a quantum liquid. Changing notations the same equation describes light propogation in a medium with Kerr nonlinearity.
[12] S. L. Rolston and W. D. Phillips, Nature (London) **416**, 219 (2002).
[13] L. Salasnich, A. Parola, and L. Reatto, Phys. Rev. A **64**, 023601 (2001).
[14] Y. Shin, M. Saba, T. A. Pasquini, W. Ketterle, D. E. Pritchard, and A. E. Leanhardt, Phys. Rev. Lett. **92**, 050405 (2004).
[15] L. D. Carr, M. J. Holland, and B. A. Malomed, J. Phys. B **38**, 3217 (2005).
[16] T. Frisch, Y. Pomeau, and S. Rica, Phys. Rev. Lett. **69**, 1644 (1992).
[17] J. E. Williams and M. J. Holand, Nature (London) **568**, 401 (1999).
[18] M. R. Matthews, B. P. Anderson, P. C. Haljan, D. S. Hall, C. E. Wieman, and E. A. Cornell, Phys. Rev. Lett. **83**, 2498 (1999).
[19] K. W. Madison, F. Chevy, W. Wohlleben, and J. Dalibard, Phys. Rev. Lett. **84**, 806 (2000).
[20] S. Inouye, S. Gupta, T. Rosenband, A. P. Chikkatur, A. Gorlitz, T. L. Gustavson, A. E. Leanhardt, D. E. Pritchard, and W. Ketterle, Phys. Rev. Lett. **87**, 080402 (2001).
[21] S. K. Adhikari, Phys. Rev. A **65**, 033616 (2002).
[22] S. A. Morgan, R. J. Ballagh, and K. Burnett, Phys. Rev. A **55**, 4338 (1997).
[23] W. P. Reinhardt and C. W. Clark, J. Phys. B **30**, L785 (1997).
[24] A. D. Jackson, G. M. Kavoulakis, and C. J. Pethick, Phys. Rev. A **58**, 2417 (1998).
[25] A. E. Muryshev, H. B. van Linden van den Heuvell, and G. V. Shlyapnikov, Phys. Rev. A **60**, R2665 (1999).
[26] R. Dum, J. I. Cirac, M. Lewenstein, and P. Zoller, Phys. Rev. Lett. **80**, 2972 (1998).
[27] S. Burger, K. Bongs, S. Dettmer, W. Ertmer, K. Sengstock, A. Sanpera, G. V. Shlyapnikov, and M. Lewenstein, Phys. Rev. Lett. **83**, 5198 (1999).
[28] J. Denschlag, J. E. Simsarian, D. L. Feder, C. W. Clark, L. A. Collins, J. Cubizolles, L. Deng, E. W. Hagley, K. Helmerson, W. P. Reinhardt, S. L. Rolston, B. I. Schneider, and W. D. Phillips, Science **287**, 97 (2000).
[29] R. J. Dodd, M. Edwards, C. J. Williams, C. W. Clark, M. J. Holland, P. A. Ruprecht, and K. Burnett, Phys. Rev. A **54**, 661 (1996).
[30] F. Dalfovo and S. Stringari, Phys. Rev. A **53**, 2477 (1996).
[31] P. A. Ruprecht, M. J. Holland, K. Burnett, and M. Edwards, Phys. Rev. A **51**, 4704 (1995).
[32] V. M. Pérez-García, H. Michinel, and H. Herrero, Phys. Rev. A **57**, 3837 (1998).
[33] L. Khaykovich, F. Schreck, G. Ferrari, T. Bourdel, J. Cubizolles, I. D. Carr, Y. Castin, and C. Salomon, Science **296**, 1290 (2002).
[34] K. E. Strecker, G. B. Partridge, A. G. Truscott, and R. G. Hulet, Nature (London) **417**, 150 (2002).
[35] G. D. Montesinos, V. M. Pérez-García, and H. Michinel, Phys. Rev. Lett. **92**, 133901 (2004).
[36] H. Saito and M. Ueda, Phys. Rev. Lett. **90**, 040403 (2003).
[37] P. G. Kevrekidis, B. A. Malomed, D. J. Frantzeskakis, and R. Carretero-González, Phys. Rev. Lett. **93**, 080403 (2004).
[38] J.-P. Martikainen and H. T. C. Stoof, Phys. Rev. Lett. **93**, 070402 (2004).
[39] T. J. Alexander, A. A. Sukhorukov, and Yu. S. Kivshar, Phys. Rev. Lett. **93**, 063901 (2004).
[40] R. Kanamoto, H. Saito, and M. Ueda, Phys. Rev. Lett. **94**, 090404 (2005).
[41] B. P. Anderson and M. A. Kasevich, Science **27**, 1686 (1998).
[42] Y. Yasui, T. Takaai, and T. Ootsuka, J. Phys. A **34**, 2643 (2001).
[43] L. D. Carr and J. Brand, Phys. Rev. Lett. **92**, 040401 (2004).
[44] S. Sinha, A. Y. Cherny, D. Kovrizhin, and J. Brand, Phys. Rev. Lett. **96**, 030406 (2006).
[45] L. Salasnich, Phys. Rev. A **70**, 053617 (2004).
[46] M. Segev, G. C. Valley, B. Crosignani, P. DiPorto, and A. Yariv, Phys. Rev. Lett. **73**, 3211 (1994); Z. Chen, M. Segev, S. R. Singh, T. Coskun, and D. N. Christodoulides, J. Opt. Soc.

Am. B **14**, 1407 (1997).
[47] Z. Dutton, M. Budde, C. Slowe, and L. V. Hau, Science **293**, 663 (2001).
[48] W. Wan, S. Jia, and J. W. Fleischer, Nat. Phys. **3**, 46 (2007).
[49] F. S. Cataliotti, S. Burger, C. Fort, P. Maddaloni, F. Minardi, A. Trombettoni, A. Smerzi, and M. Inguscio, Science **293**, 843 (2001).
[50] E. Madelung, Z. Phys. **40**, 322 (1927).
[51] J. H. Marburger, Prog. Quantum Electron. **4**, 35 (1975).
[52] Y. Silberberg, Opt. Lett. **15**, 1282 (1990).
[53] O. S. Rozanova, Proc. Am. Math. Soc. **133**, 2347 (2005).
[54] Fanghua Lin and Ping Zhang (private communication).
[55] R. Carles, Commun. Math. Phys. **269**, 195 (2007).
[56] V. Fleurov and A. Soffer, Europhys. Lett. **72**, 287 (2005).
[57] M. A. Hoefer, M. J. Ablowitz, I. Coddington, E. A. Cornell, P. Engels, and V. Schweikhard, Phys. Rev. A **74**, 023623 (2006).
[58] E. Bettelheim, A. G. Abanov, and P. Wiegmann, Phys. Rev. Lett. **97**, 246401 (2006).
[59] A. A. Abrikosov, Dokl. Akad. Nauk SSSR **86**, 489 (1952).
[60] S. Bar-Ad (private communication); see also D. Cheskis, S. Bar-Ad, R. Morandotti, J. S. Aitchison, H. S. Eisenberg, Y. Silberberg, and D. Ross, Phys. Rev. Lett. **91**, 223901 (2003).
[61] D. Mandelik, Y. Lahini, and Y. Silberberg, Phys. Rev. Lett. **95**, 073902 (2005).
[62] Z. Schuss, *Theory and Application of Stochastic Differential Equations* (Wiley, New York, 1980).
[63] E. H. Hauge and J. A. Støvneng, Rev. Mod. Phys. **61**, 917 (1989).
[64] L. A. Maccoll, Phys. Rev. **40**, 621 (1932).
[65] E. Pollak and W. H. Miller, Phys. Rev. Lett. **53**, 115 (1984).
[66] P. Balcou and L. Dutriaux, Phys. Rev. Lett. **78**, 851 (1997).
[67] M. Büttiker and R. Landauer, Phys. Rev. Lett. **49**, 1739 (1982).
[68] G. B. Whitham, *Linear and Nonlinear Waves* (Wiley, New York, 1974).
[69] A. Soffer and M. I. Weinstein, Phys. Rev. Lett. **95**, 213905 (2005).
[70] A. Soffer and C. Stucchio, the program is available online at http://www.math.rutgers.edu/~stucchio/software/kitty/Kitty.html
[71] J. Holmer, J. Marzuola, and M. Zworski (unpublished).
[72] Z. Nussinov and S. Nussinov, e-print cond-mat/0409094.
[73] L. D. Carr and Y. Castin, Phys. Rev. A **66**, 063602 (2002).